

Effect of lane allocation on operational efficiency at weaving areas based on a cellular automaton model

Xu An¹, Jing Zhao¹✉, Peng Li², Xiaodan Ma¹

¹Department of Traffic Engineering, University of Shanghai for Science and Technology, 516 Jungong Road, Shanghai, People's Republic of China

²Department of Supply Chain Management, Rutgers University, The State University of New Jersey, Newark, NJ, USA

✉ E-mail: jing_zhao_traffic@163.com

ISSN 1751-956X

Received on 17th April 2018

Revised 30th November 2018

Accepted on 2nd January 2019

E-First on 11th January 2019

doi: 10.1049/iet-its.2018.5143

www.ietdl.org

Abstract: The traffic weaving area is one of the key bottlenecks affecting the operation efficiency of an urban expressway system. The main motivation of this study is to explore the effects of lane allocation on the operational efficiency at weaving areas. A cellular automaton model was established, in which three different lane-changing rules were considered to match the driving behaviour when the lanes are allocated. Using the average vehicular travel time and the average velocity as the indicators, the operational performance of various lane allocation schemes was compared under different traffic and geometric conditions. A case study is used to validate and evaluate the effectiveness of the proposed method. The results show that the benefits of the lane-allocation strategy are affected by the traffic flow, weaving volume ratio, weaving length, and installation location of the isolation facilities. The lane-allocation strategy has promising application under the conditions of a traffic flow that is >400 veh/in, at weaving volume ratio between 0.2 and 0.7, and weaving length shorter than 300 m. Moreover, the isolation facilities should cover the weaving area when the lane-allocation strategy is used.

1 Introduction

The traffic weaving area is one of the key bottlenecks that affects the operation efficiency of an urban expressway system. It is formed when the merge area is followed by a diverge area or when an on-ramp is followed by an off-ramp, and there is an auxiliary lane connection between them. The factors that influence the traffic efficiency in the weaving area of an urban expressway include the traffic flow pattern [1, 2], speed [3–5], weaving area length [2, 4, 5], acceleration lane length [5, 6], exclusive bus lane [7, 8], guide sign [9], and lane-changing behaviour [5, 10–14]. In order to reduce the congestion at the weaving area, various management and control strategies were proposed [15, 16], including ramp metering (RM) [17–19], variable speed limit (VSL) [20], integrated RM and VSL (RM-VSL) [21, 22], high-occupancy/toll lanes [23, 24], route guidance [25], and lane allocation [26].

Among these strategies, lane allocation is a method for improving the running order of the weaving area, which could segregate drivers by destination and force them to change lanes only where allowed. Daganzo [26] proposed the use of a lane-assignment strategy at the off ramp. It was found that assigning multiple lanes to exiting traffic can alleviate the queuing from affected upstream ramps. Wang *et al.* [27] expanded the use of the lane-assignment strategy to freeway weaving areas. An optimal lane-assignment model was proposed for one-sided freeway weaving areas to reduce the disturbance between weaving and non-weaving traffic streams. The results showed that the lane-allocation strategy could increase the capacity of the weaving area under certain on-ramp volume and weaving volume ratios and decrease the traffic delay. Zhao *et al.* [28] further proposed an integrated optimisation model that explicitly took into consideration the two optimisation strategies, namely the lane allocation and on-ramp signal control, and their combinations.

Reasonable lane allocation can allow the traffic to flow in a more orderly manner. However, in the existing studies, it is assumed that the capacity is given and will not change even under over-saturated conditions. The analytical models that consider lane allocation in weaving areas and the corresponding operation benefit analysis are relatively lacking.

In existing studies, a series of analytical models were established based on traffic flow theory [29–35]. In the research on the traffic flow of the weaving area, the modelling methods used include the regression model [36, 37], car-following model [38–40], and cellular automaton (CA) model [41, 42]. The CA model is a commonly used modelling method that represents the evolution of states through mapping and can simulate the state of space time [43–47]. There is a large body of research on the CA model for simulating urban expressway operation. Wang *et al.* [48] investigated the effects of passing lanes on traffic flow on a single-lane highway based on a CA model. The traffic flow conditions under different flow rates and different operating lengths were analysed. Rassafi *et al.* [49] modelled a drivers' behaviour on a basic freeway by nesting the logit model simulation rules into the CA model. The existing systems showed that focused drivers select their next position in accordance with the maximum safe speed. In order to more realistically reflect real-world vehicular movement, Lan *et al.* [50] proposed a piecewise linear movement to replace the conventional particle-hopping movement adopted in previous CA models. The model can be used to reveal Kerner's three-phase traffic patterns and the phase transitions among them. Lv *et al.* [51] extended the continuous single-lane models to simulate lane-changing behaviour on an urban roadway that consists of three lanes. The effects of the lane-changing behaviour on the distribution of vehicles, velocity, flow, and headway were investigated.

This study aims to establish a CA model to explore the effects of lane allocation on the operational efficiency at weaving areas, by which the operational situation under high saturation can be modelled more realistically. Three different lane-changing rules are considered to match the driving behaviour when the lanes are allocated. Using the average vehicular travel time and the average velocity as the main indicators, the operational performance under various lane-allocation schemes for one-sided weaving areas (A-type weaving area in HCM2010 [52]) were compared and application recommendations were provided.

The rest of this paper is organised as follows. In Section 2, the CA model is established with the consideration of lane allocation at weaving areas. Extensive numerical simulation analyses are conducted in Section 3 to explore the effect of the lane allocation

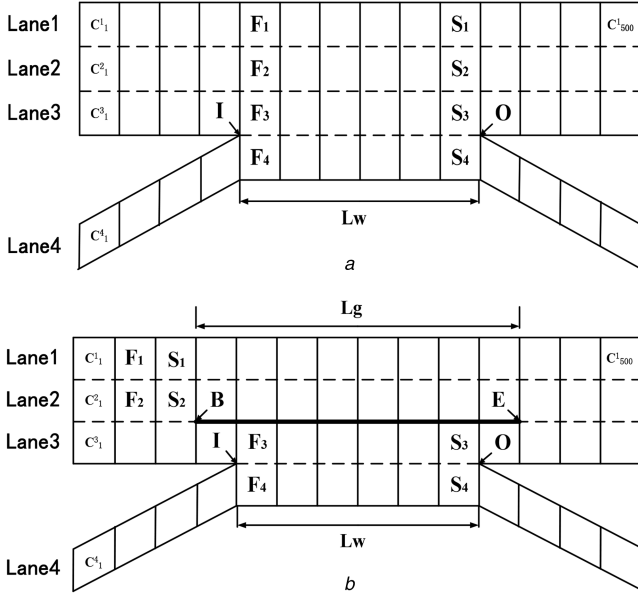


Fig. 1 Weaving area description

(a) Scheme 1: without the isolation facility, (b) Scheme 2: with installed isolation facilities. Note: C_i^n is the cell position; n is the lane number; i is the cell number; F_n is the start of the judging position of the weaving area; S_n is the end of the judging position of the weaving area; I is the beginning of the weaving area; O is the end of the weaving area; B is the beginning of the isolation facility; E is the end of the isolation facility; L_w is the length of the weaving area; and L_g is the length of the isolation facility

strategy on the traffic flow at weaving areas and to identify its best applications. Conclusions are presented at the end of the paper.

2 Model

The weaving area comprises multiple streams running in different directions. The driving behaviour in the weaving area includes car following and lane changing.

The A-type weaving area with three lanes for the main road and one lane for the on-ramp and off-ramp is studied, as shown in Fig. 1. Two schemes of lane allocation are considered. Fig. 1a shows the scheme without an isolation facility, while Fig. 1b shows the scheme with isolation facilities installed. The lane-allocation strategy splits the lanes in the weaving area into two parts: one designated for the through traffic only (through traffic only part) and the other assigned to the weaving traffic (weaving traffic part).

The travel of the vehicle is modelled as a cellular transmission. In Fig. 1, each cell has two states: 0 and 1. State 0 indicates that the cell is empty, while state 1 indicates that the cell is occupied by a car. The length of the weaving area is denoted by L_w , that is $[I, O]$ in Fig. 1. The length of the isolation facility is denoted by L_g , that is $[B, E]$ in Fig. 1. The cellular transmission runs based on the iteration with one unit of time in each step. The operational rules include direct rules and lane-changing rules.

2.1 Car following rules

Car following rules are based on the Nagel–Schreckenberg (NS) model [53, 54]:

- Acceleration: when $v_n(t) < V$, $v_n(t)$ increases by 1. $v_n(t) = v_n(t) + 1$.
- Braking: when $v_n(t) > g_n(t)$, $v_n(t)$ drops to $g_n(t)$. $v_n(t) = g_n(t)$.
- Randomisation: $v_n(t)$ decreases by 1 with the probability p . $v_n(t) = v_n(t) - 1$ (p is the probability of randomisation).
- Driving: the above steps 1–3 are used to update the position. It is the configuration at time $t + 1$. $x_n(t + 1) = x_n(t) + v_n(t)$.

where $v_n(t)$ is the speed of the n th vehicle at time t , $v_n(t) \in [0, V]$, V is the maximum speed of the vehicle, $V = v_{\max}$ for the vehicles in the weaving area, $V = v_{\max}'$ for the vehicles in other areas, $g_n(t) = x_{n-1}(t) - x_n(t) - 1$ is the number of empty cells in front of the n th vehicle at time t , and $x_n(t)$ is the position of the n th vehicle at time t .

The system operation requires an initial condition; the specific conditions are as follows:

- Initial position of vehicles. Vehicles enter the initial cell of the lanes on the main road (C_1^1 – C_1^3) and the initial cell of the lanes on the on-ramp (C_4^4) with a certain flow rate.
- Initial velocity of vehicles. The initial velocity of each vehicle is V .
- Initial destination of vehicles. The destination of each vehicle is given when it enters the system. Among all the vehicles entering from the main road, the ratio of the vehicles heading for the off-ramp is α_1 . Among all the vehicles entering from the on-ramp, the ratio of the vehicles heading for the main road is α_2 . The vehicle disappears in the system after travelling through the lane terminal cells.

2.2 Lane-changing rules

Three types of lane-changing rules are developed in accordance with the strength of the lane change demand, namely strong demand lane change rule, moderate demand lane change rules, and weak demand lane change rules. They are applied in different areas.

- The strong demand lane change rule is applied to the weaving area ($[F_i, S_j]$ area), where the vehicles on the main road (lanes 1, 2, and 3) need to enter lane 4, and the vehicles on lane 4 need to enter the main road, as shown in Fig. 1. The criteria for a strong demand lane change are that if (1) and (2) are satisfied, the vehicle changes lanes immediately. This indicates that the effect of the lane change on the current vehicle is not taken into consideration. The vehicle must be moved to the target lane immediately, or it will have to wait at the end of the weaving area, cell S_4 . Equation (1) shows that the speed of the vehicle after changing lanes is not taken into consideration. Equation (2) shows that the effect of the lane change on the vehicle in the target lane is not taken into consideration:

$$g_i^- \geq g_i, \text{ or } g_i^- \geq 1 \quad (1)$$

$$g_i^+ \geq g_i, \text{ or } g_i^+ \geq 1 \quad (2)$$

where g_i is the number of empty cells between the current lane target vehicle and the vehicle in front of the target vehicle, g_i^- is the number of empty cells between the vehicle and the vehicle behind at the adjacent target lane, and g_i^+ is the number of empty cells between the vehicle and the vehicle travelling ahead in the adjacent target lane.

- The moderate demand lane change rule is applied to the weaving preparation area ($[C_i, F_i]$ area), where the vehicles are prepared to enter into the weaving area by changing the lane in advance. The criteria for moderate lane change are that if (3) and (4) are satisfied, the vehicle changes lanes immediately. If this condition cannot be satisfied, the vehicle will be stopped at the S_1 or S_2 cells in Fig. 1 and will change lanes until the conditions are met. Equation (3) indicates that lane change should not affect the vehicle travelling behind in the target lane. Equation (4) shows that although the current lane change demand is medium, it is still necessary to change to the target lane as soon as possible without considering the impact on the current vehicle speed after the lane change:

$$g_i^- \geq \min \{v_i^- + 1, V\} \quad (3)$$

$$g_i^+ \geq g_i \text{ or } g_i^+ \geq 1 \quad (4)$$

where v_i is the target vehicle speed and v_i^- is the speed of the vehicle travelling behind in the target lane.

- iii. The weak demand lane change rule is applied to the vehicles in all areas in order to obtain a higher speed. It is the weakest lane change demand. Vehicles that meet the weak lane-changing rule will change lanes with a certain probability p_c . The condition for judging the lane change is whether (5)–(7) are satisfied. The lane change rule (3) indicates the need to consider the effect of lane change on the target vehicle itself and the vehicle behind the target vehicle. Equation (5) indicates that lane changing of the target vehicle should not affect the movement of the vehicle behind and in the adjacent target lane. Equations (6) and (7) indicate that the vehicle in front affects the driving of the target vehicle, and the target vehicle can achieve a higher speed after changing to the target lane without affecting the driving of the vehicle travelling behind in the target lane:

$$g_i^- \geq \min \{v_i^- + 1, V\} \quad (5)$$

$$g_i < \min \{v_i + 1, V\} \quad (6)$$

$$g_i^+ \geq \min \{v_i + 1, V\} \quad (7)$$

Lane change rules correspond to the lane change situation as shown in Fig. 2. In the following lane-changing rules, A–D correspond to strong demand lane change areas, E–H correspond to medium demand lane change areas, and I–L correspond to weak demand lane change areas.

- a. In the strong demand lane change area, if the ahead cell is empty at the current lane and the number of empty cells ahead on the target lane is <1 , the vehicle will not change lanes at this step.
- b. If the ahead cell is empty in the current lane and the back cell on the target lane is occupied, the vehicle will not change lanes at this step.
- c. If the ahead cell is empty in the current lane and the ahead and back cells on the target lane are not occupied, the vehicle can change lanes.
- d. If the cell in front of the vehicle is occupied, the vehicle can change lanes as long as no vehicle exits at the parallel cell in the target lane.
- e. In the moderate demand lane change area, if the ahead cell is empty in the current lane and the number of empty cells ahead in the target lane is <1 , the vehicle will not change lanes at this step.
- f. If the cell in front of the vehicle is occupied and the number of empty back cells in the target lane is less than the safe gap, the vehicle will not change lanes at this step.
- g. If the ahead cell is empty in the current lane, the vehicle can change lanes when the ahead cell in the target lane is not occupied and the number of empty back cells in the target lane is greater than the safe gap.
- h. If the cell in front of the vehicle is occupied, the vehicle can change lanes when the number of empty back cells in the target lane is greater than the safe gap.
- i. In the weak demand lane change area, if the promised speed in the target lane is less than that of the current lane, the vehicle will not change lanes at this step.
- j. If the number of empty back cells in the target lane is less than the safe gap, the vehicle will not change lanes at this step.
- k. If the promised speed in the current lane reaches the maximum velocity, the vehicle will not change lanes at this step.
- l. The vehicle can change lanes if the promised speed in the target lane is greater than that of the current lane and the

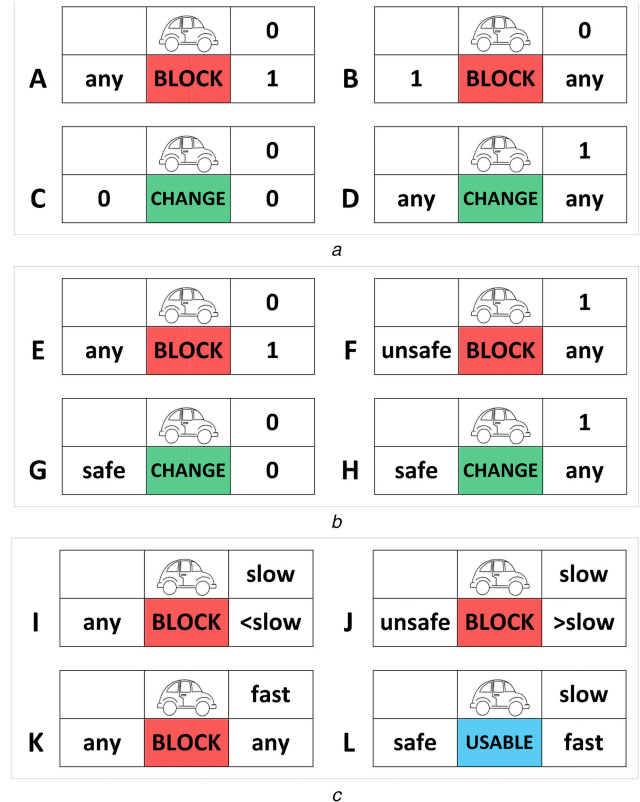


Fig. 2 Lane-changing rules

(a) Rules in strong demand lane change area, (b) Rules in moderate demand lane change area, (c) Rules in weak demand lane change area. Note: BLOCK means vehicle cannot change lanes; CHANGE means vehicle will change lanes; USABLE means vehicle will change lanes with a certain probability

Table 1 Cell size

Type	Length		Width	
	Size, m	Cell	Size, m	Cell
one cell	5	1	3.5	1
entire region	2500	500	14	4
statistics region	1500	300	14	4

number of empty back cells in the target lane is greater than the safe gap.

3 Simulations and analyses

Each lane in the simulation system contains 500 cells numbered from 1 to 500. The probability of random moderation used in the straight rules, p , is set to be 0.33; the probability of weak demand lane changing, p_c , is 0.2; the maximum velocity is 2 in the weaving area and 3 in the other area; the single-lane saturated flow $Q = 1000$ veh/lane. The data obtained during the simulation steps 400–900 in sections C_{100}^i to C_{400}^i are collected for analysis in order to exclude the impact of vehicles at the front and rear of the system. Specific cell size information is listed in Table 1. According to the above parameters for the simulation, all the following analysis data are average values of 50 runs.

In order to analyse the effect of the lane-allocation strategy, four factors are considered: the traffic flow (total demand flow rate in the weaving segment), weaving volume ratio (the ratio of weaving flow rate to total flow rate in the weaving segment), weaving length (length of the interwoven section from the import triangle to the exit triangle), and the installation location of isolation facilities. The parameters used in the model are defined as follows: weaving length L_w is 20, isolation facility length L_g is 30, isolation facilities starting position B is 235, weaving area starting position I is 240, traffic flow is 700 veh/in, and weaving volume ratio α is 0.2.

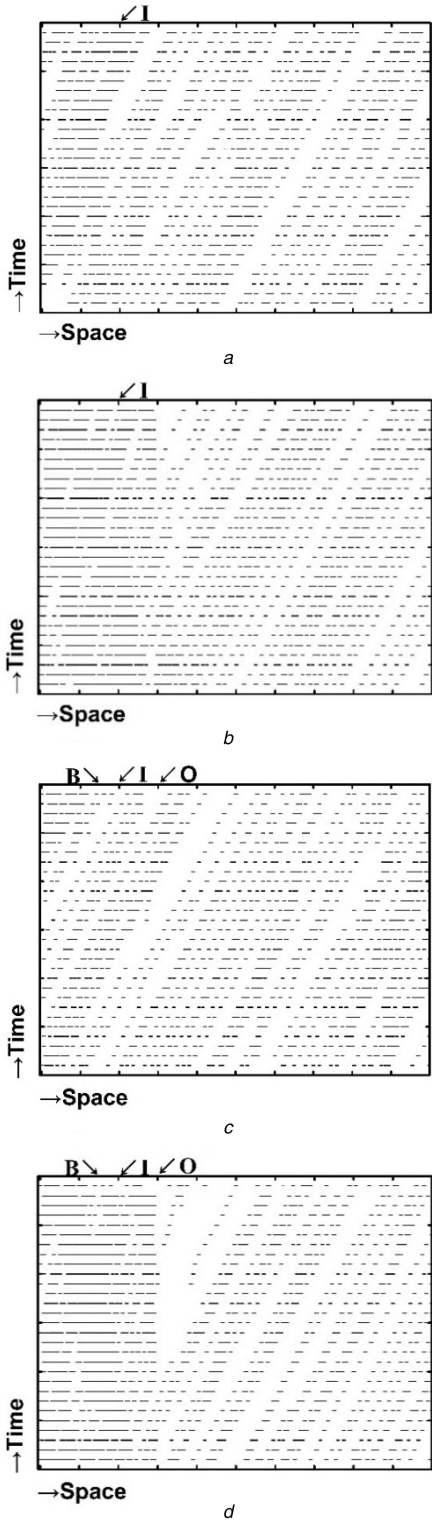


Fig. 3 Space-time pattern of two lane allocation schemes

(a) Lane 2 in scheme 1, (b) Lane 3 in scheme 1, (c) Lane 2 in scheme 2, (d) Lane 3 in scheme 2. Note: B is the beginning of the isolation facility; I is the beginning of the weaving area; O is the end of the weaving area

3.1 Effect of traffic flow

The space-time patterns of two-lane allocation schemes are shown in Fig. 3. The phenomenon of vehicle track interruption appears to be reasonable owing to the lane change factor, t . Under scheme 1, crowded waves spread slightly backwards in lane 2, while the traffic flow runs smoothly under scheme 2.

Fig. 4 shows the operational state of the weaving and the non-weaving areas under the change in the main road and on-ramp single-lane flow rate. The traffic flow is set in the range of 0–1000 veh/in. According to the code for design of urban road engineering

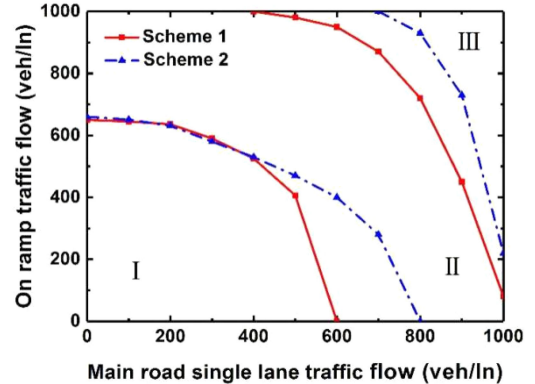


Fig. 4 Operational state under various traffic flows

[55], the average vehicle speed of two cells is used as the phase-transition point. Area I indicates that both the weaving area and the non-weaving area are non-crowded, Area II indicates that the weaving area is crowded but the non-weaving area is non-crowded, and Area III indicates that both the interleaved area and the non-interleaved area are crowded. As shown in Fig. 4, in the comparison of scheme 1, Area I is enlarged in scheme 2 and Area III is reduced. The dividing lines of scheme 2 are then moved to the right according to the comparison with scheme 1. This indicates that scheme 2 outperforms scheme 1 in a majority of the tested cases. Moreover, obvious improvement can be obtained when the traffic flow of the main road is >400 veh/in. This indicates that the setting of the isolation facilities has a wider application range when the traffic flow is high.

In order to analyse the influence of schemes 1 and 2 on the traffic flow of different paths, Fig. 5 further shows the travel time for four paths, which includes the paths from the main line to the main lane, the main line to the off-ramp, the on-ramp to the off-ramp, and the on-ramp to the main line. Fig. 5c shows the percentage of reduction of travel time for scheme 2 in comparison with scheme 1, in which the negative values indicate that the travel time in scheme 2 is higher than that in scheme 1. When the traffic flow is <400 veh/in, the performance of the two schemes is comparable. When the traffic flow is between 400 and 500 veh/in, the travelling times of the four paths in scheme 2 are shorter than those of scheme 1. When the traffic flow is >500 veh/in, the vehicle travel time increases rapidly, indicating that the weaving area begins to become crowded, which is consistent with the results of Fig. 4. Scheme 2 can effectively separate weaving vehicles from non-weaving vehicles by using the lane-allocation strategy, and the travel time of the vehicles from the main road is obviously shortened. However, the travel time of the on-ramp vehicles may be increased owing to the increase in the weaving volume ratio. Fig. 5c shows that the reduction (positive value) in the travel time for vehicles from the main road is significantly greater than the increase (negative value) in the travel time for vehicles from the on-ramp. Overall, scheme 2 improves the operational efficiency by 13.6% on average when the traffic flow is >500 veh/in.

3.2 Effect of the weaving volume ratio

In order to explore the impact of the weaving volume ratio on the operation of the two schemes, the phase change of the system is first analysed, as shown in Fig. 6. The weaving volume ratio is set in the range of 0–1. It can be observed that, when the ratio of the vehicles heading for the main road among all the vehicles entering from the on-ramp (α_2) is <0.7, the dividing line between Areas II and III of scheme 2 is higher than that of scheme 1. This indicates that scheme 2 can alleviate the congestion in the non-weaving area when α_2 is <0.7. Similarly, scheme 2 can alleviate the congestion in both the weaving and non-weaving areas when α_2 is <0.4. Moreover, it can be observed that the lane-changing probability of the main road is a more critical factor for the operational state of the weaving area as compared to the lane-changing probability of the on-ramp. This is mainly because the main road commonly has a higher traffic flow.

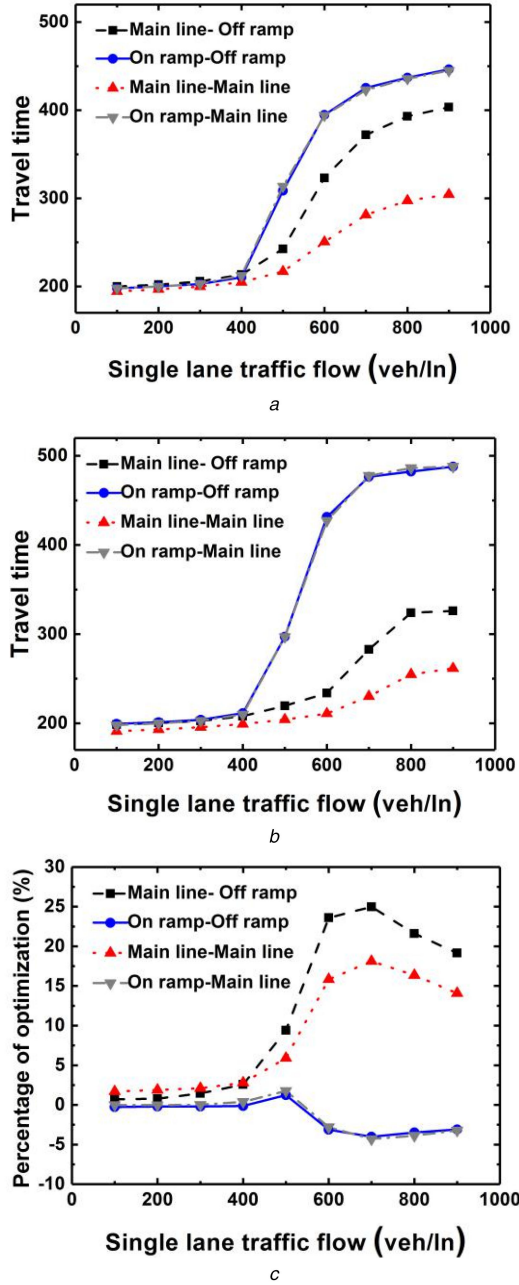


Fig. 5 Travel time for the four paths under the different traffic flows
(a) Scheme 1, (b) Scheme 2, (c) Reduction percentage of scheme 2 over scheme 1

The travel time of the four paths are compared, as shown in Fig. 7. For the path from the main line to the main line, the reduction percentage of the travel time obtained with scheme 2 first increases and then reaches a platform with the increase in the weaving volume ratio. This is because scheme 2 can effectively separate the weaving vehicles from the non-weaving vehicles by using the lane-allocation strategy. For the weaving paths (main line to off-ramp and on-ramp to main line), scheme 2 can reduce the travel time when the weaving volume ratio is low (<0.7) while the travel time increases when the weaving volume ratio is high (>0.7). This is because the operational order can be improved with the installation of isolation facilities. However, as the installation of isolation facilities reduces the number of lanes used for weaving, when the weaving volume ratio is high, the capacity of the lanes in the weaving section is lower than the weaving volume, which causes a reduction in the operational efficiency. Therefore, it should be ensured that under-saturation conditions exist in the weaving traffic part in the weaving area when applying the lane-allocation strategy.

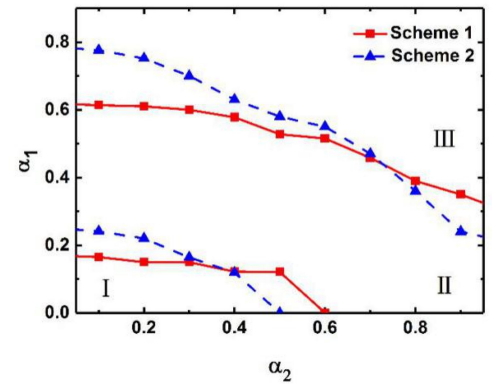


Fig. 6 Operational state under different weaving volume ratio

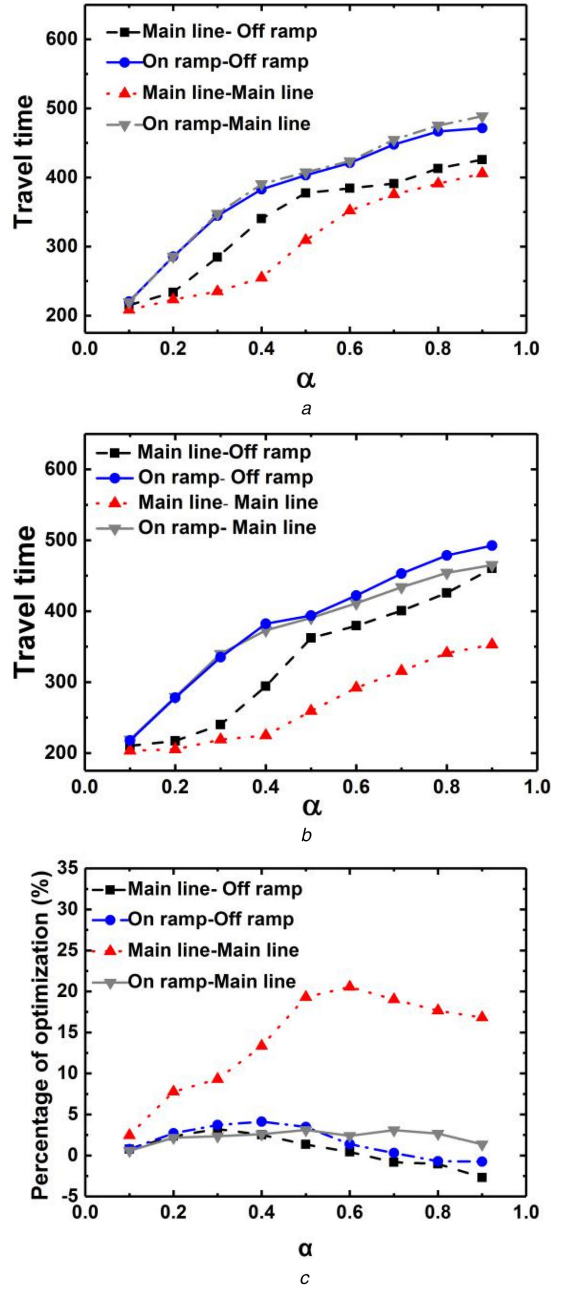


Fig. 7 Travel time of the four paths under different weaving volume ratio
(a) Scheme 1, (b) Scheme 2, (c) Reduction percentage of scheme 2 over scheme 1

3.3 Effect of weaving length

In order to explore the impact of the weaving length on the operation of the two schemes, the average velocity (V), average

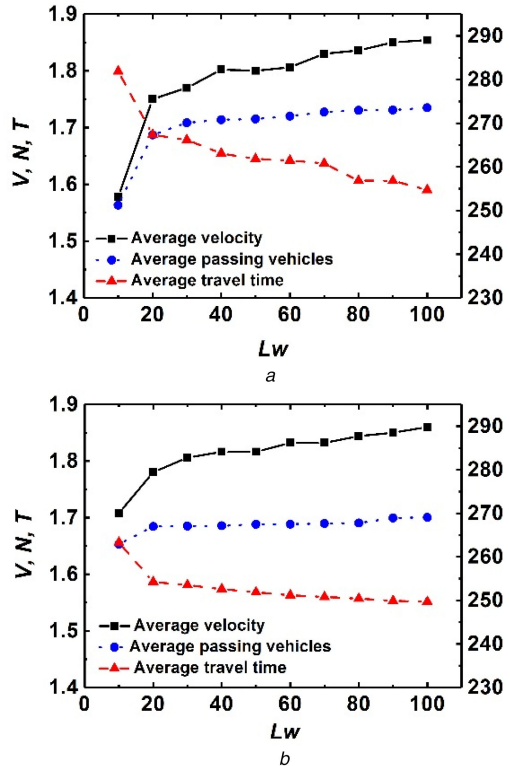


Fig. 8 Operational efficiency under different weaving area lengths
(a) Scheme 1, (b) Scheme 2

throughput (N), and average travel time (T) are analysed under different weaving lengths, as shown in Fig. 8. With the increase in the length of the weaving area, the travelling speed and throughput of schemes 1 and 2 increase, while the travel time of the two schemes decreases. In general, scheme 2 outperforms scheme 1 in all the three indicators. This outperformance is more significant when the weaving length is short. When the weaving length is >60 cells (300 m), the performance of scheme 1 and that of scheme 2 tend to be the same. This indicates that the benefits of the lane-allocation strategy are more pronounced when the length of the weaving area is short. This is because the operation of complex movements cannot be smoothly organised in the weaving area, and the lane-allocation strategy can be used to standardise the traffic flow of different movements. With the increase in the weaving length, the self-organising ability of the weaving area improves. Therefore, there is no need to use the lane-allocation strategy. Overall, scheme 2 improves the operational efficiency by 8.3% on average when weaving length is <300 m.

3.4 Effect of the installation location of isolation facilities

The installation location of isolation facilities also plays an important role in affecting the performance of the lane-allocation strategy. According to Fig. 1, the isolation facilities can be located between lanes 1 and 2 (scheme 2–1) and between lanes 2 and 3 (scheme 2–2).

The average vehicle travel time and average travel speed under scheme 2–1 and 2–2 are compared, as shown in Fig. 9. For each sub-figure, the horizontal and vertical axes represent the length and starting location of the isolation facilities, respectively, and the contour lines illustrate the travel time and speed. The travel time reduces and travel speed increases with the increase in the length and starting location of the isolation facilities. Comparing the schemes that the isolation facilities cover the entire weaving area and not cover the entire weaving area, the former can obtain 10.1% reduction in travel time on average.

Fig. 10 further analyses the performance of the two-lane allocation schemes under different volume patterns. When the ratio of the vehicles heading for the off-ramp among all the vehicles entering from the main road (α_1) is greater than the weaving volume ratio of the traffic flow from the on-ramp (α_2), i.e. $\alpha_1 = 5\alpha_2$,

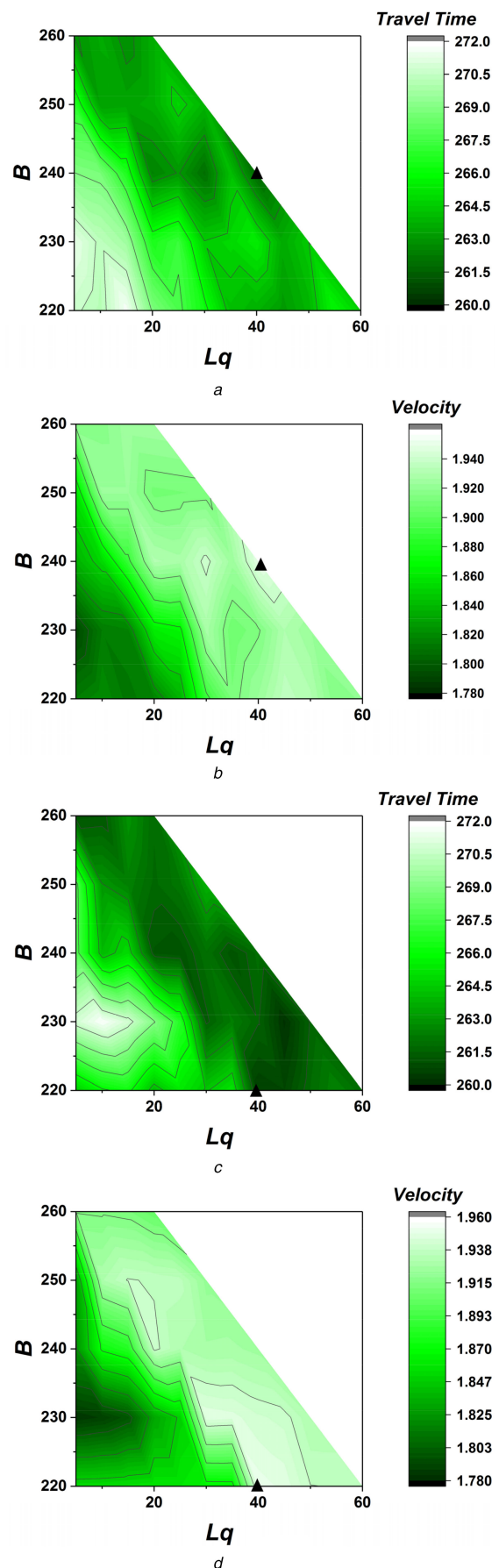


Fig. 9 Comparison of lane location scheme 2–1 and 2–2
(a) Travel time for scheme 2–1, (b) Velocity for scheme 2–1, (c) Travel time for scheme 2–2, (d) Velocity for scheme 2–2

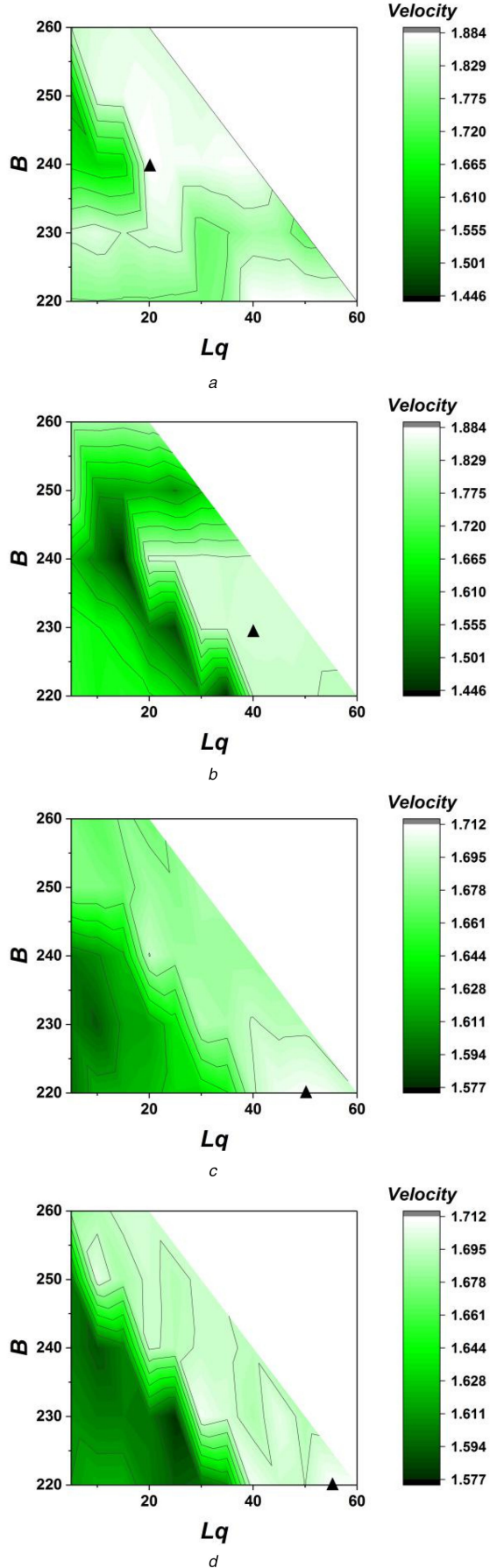


Fig. 10 Travel speed comparison of the lane-allocation scheme 2-1 and 2-2 under different weaving volume ratios
 (a) Scheme 2-1 when $\alpha_1 > \alpha_2$, (b) Scheme 2-2 when $\alpha_1 > \alpha_2$, (c) Scheme 2-1 when $\alpha_2 > \alpha_1$, (d) Scheme 2-2 when $\alpha_2 > \alpha_1$

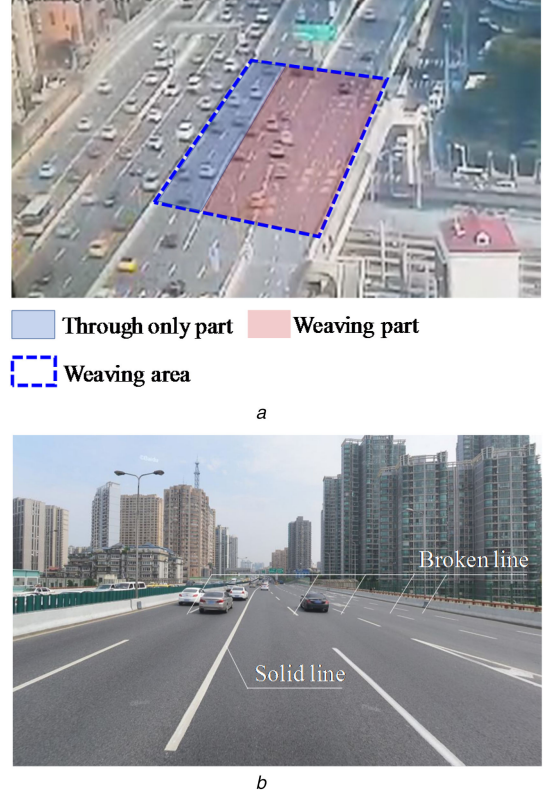


Fig. 11 Geometric layout of the study site
 (a) Case study weaving area, (b) Lane markings

as shown in Fig. 10, the average travel speed of the weaving area under scheme 2-1 is generally higher (3.2% on average) than that of scheme 2-2. Therefore, the isolation facilities should be located between lanes 1 and 2 when $\alpha_1 > \alpha_2$. When α_2 is greater than α_1 , the average travel speed of the weaving area under scheme 2-2 is generally greater (2.6% on average) than that of scheme 2-1. Therefore, the isolation facilities should be located between lanes 2 and 3.

4 Case study

A weaving area on the N-S Elevated Road (from Tianmu Road to Yongxing Road) in Shanghai, China, is used to validate and evaluate the effectiveness of the proposed method, as illustrated in Fig. 11a. There are four main lanes with three on-ramp lanes and three off-ramp lanes. The length of the weaving area L_w is 115 m (23 cells). Scheme 2-2 have been used in the study site in reality. The inside two lanes of the main-line are designated for the through traffic only (through traffic only part) and the other five lanes are assigned to the weaving traffic (weaving traffic part). The two parts are separated by setting solid line marking, as shown in Fig. 11b.

The traffic operation data, including traffic volume, travel speed, and lane-changing movements, from 7:00 to 14:00 were collected by video camera. The ratio of the vehicles heading for the off-ramp among all the vehicles entering from the main road (α_1) is 0.19, and the ratio of the vehicles heading for the main road among all the vehicles entering from the on-ramp (α_2) is 0.27. Input these parameters into the proposed CA model, using the average speed as the indicator; the comparison results are shown in Fig. 12. The data was aggregated in every 20 min.

From Fig. 12, one can observe that the performance of the proposed CA model and that of the field survey data are similar. The proposed model could cause an error under 9% in all statistical intervals. The average error is 5.17%, which shows that the accuracy of the proposed method is acceptable.

Moreover, comparing different lane-allocation schemes, it is found that when the average speed is in an extreme high or extreme low level (around 7:00 and 8:40), the setting of lane-allocation

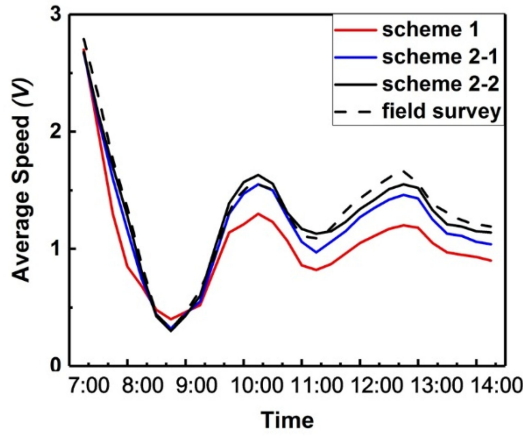


Fig. 12 Travel speed comparison of the case study

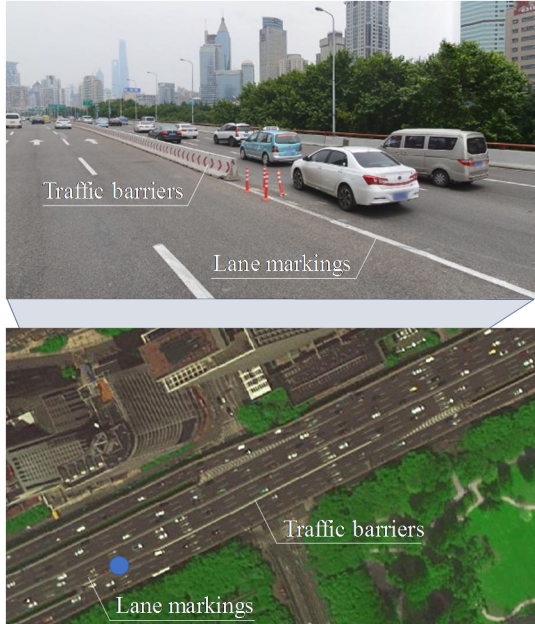


Fig. 13 Example of the setting of traffic markings and barriers in practice

facilities has little influence on the current state. It means that if the weaving area is extremely unobstructed or congested, lane-allocation schemes will lose effect, which is consistent with the above analysis. Furthermore, scheme 2–2 outperforms both scheme 2–1 and scheme 1. On average, scheme 2–2 can increase traffic speed by 12.3 and 2.7% than scheme 2–1 and scheme 1, respectively. Therefore, scheme 2–2 is applied.

In practice, to overcome the potential driving violation behaviour of lane changing at the solid line marking area [56, 57], more coercive isolation facilities, such as traffic barriers, can be used to manage the lane-changing behaviour, as shown in Fig. 13.

5 Conclusions

In this paper, a new CA model of the weaving area along with the consideration of lane allocation is established. The effects of the lane allocation on the traffic flow in weaving areas under different traffic and geometric conditions are studied by using the average travel time and average travel speed as the performance indicators. A case study is used to validate and evaluate the effectiveness of the proposed method. The results of the sensitivity analysis show that the benefits of the lane-allocation strategy are affected by the traffic flow, weaving volume ratio, weaving length, and installation location of isolation facilities. The lane-allocation strategy has promising application (~10% improvement in operational efficiency) under conditions that of high traffic flow (>400 veh/ln), medium weaving volume ratio (0.2–0.7), and short weaving length (<300 m).

Please note that the isolation facilities should cover the weaving area when the lane-allocation strategy is used. The setting of traffic markings and barriers may cause some limitations, including the flexibility of the management strategy and the drivers' reaction. However, the benefits of the lane-allocation method can be fully achieved under the connected and automated vehicles environment [58–60]. In future studies, more consideration will be given to the real-time optimisation strategy based on the real-time vehicle cooperative system.

6 Acknowledgment

The research is supported by the National Natural Science Foundation of China under grant no. 51608324.

7 References

- [1] Zhu, S., Xu, Y., Yan, Y., et al.: ‘Study on traffic safety, efficiency and intervention in weaving area’. IEEE Int. Conf. Service Operations and Logistics and Informatics, Beijing, China, 2008
- [2] Kwon, E., Lau, R., Aswegan, J.: ‘Maximum possible weaving volume for effective operations of ramp-weave areas: online estimation’, *Transp. Res.*, 2000, **1727**, pp. 132–141
- [3] Lertworawaniich, P., Elefteriadou, L.: ‘Generalized capacity estimation model for weaving areas’, *J. Transp. Eng.-ASCE*, 2007, **133**, (3), pp. 166–179
- [4] Pulugurtha, S.S., Bhatt, J.: ‘Evaluating the role of weaving section characteristics and traffic on crashes in weaving areas’, *Traffic Inj. Prev.*, 2010, **11**, (1), pp. 104–113
- [5] Wan, X., Jin, P.J., Yang, F., et al.: ‘Merging preparation behavior of drivers: how they choose and approach their merge positions at a congested weaving area’, *J. Transp. Eng.*, 2016, **142**, (9), article ID: 05016005
- [6] Luo, J., Tan, Y., Han, Y.: ‘Length design method of acceleration lane on expressway weaving area’, *Comput. Eng. Appl.*, 2015, **51**, (9), pp. 248–251
- [7] Chen, X.M., Yu, L., Jia, X.C., et al.: ‘Capacity modeling for weaving, merge, and diverge sections with median exclusive bus lanes on an urban expressway microsimulation approach’, *Transp. Res. Rec.*, 2016, **2553**, (2553), pp. 99–107
- [8] Chen, X.M., Yu, L., Zhu, L., et al.: ‘Microscopic traffic simulation approach to the capacity impact analysis of weaving sections for the exclusive bus lanes on an urban expressway’, *J. Transp. Eng. ASCE*, 2010, **136**, (10), pp. 895–902
- [9] Sun, J., Yang, X.G., Zhang, B.B., et al.: ‘Micro-simulation of urban expressway weaving sections using field data in shanghai’. 7th IEEE Int. Conf. Intelligent Transportation Systems, Washington, DC, US, 2004
- [10] Bham, G.H.: ‘A simple lane change model for microscopic traffic flow simulation in weaving sections’, *Transp. Lett. Int. J. Transp. Res.*, 2011, **3**, (4), pp. 231–251
- [11] Chen, D.J., Ahn, S.: ‘Capacity-drop at extended bottlenecks: merge, diverge, and weave’, *Transp. Res. Part B-Methodol.*, 2018, **108**, pp. 1–20
- [12] Mai, T., Jiang, R., Chung, E.: ‘A cooperative intelligent transport systems (C-ITS)-based lane-changing advisory for weaving sections’, *J. Adv. Transp.*, 2016, **50**, (5), pp. 752–768
- [13] Wan, X., Jin, P.J., Gu, H.Y., et al.: ‘Modeling freeway merging in a weaving section as a sequential decision-making process’, *J. Transp. Eng. Part B-Syst.*, 2017, **143**, (5), article ID: 05017002
- [14] Knoop, V.L., Buisson, C.: ‘Calibration and validation of probabilistic discretionary lane-change models’, *IEEE Trans. Intell. Transp. Syst.*, 2015, **16**, (2), pp. 834–843
- [15] Jiang, Z.T., Chen, X.Q., Ouyang, Y.F.: ‘Traffic state and emission estimation for urban expressways based on heterogeneous data’, *Transp. Res. Part D-Transp. Environ.*, 2017, **53**, pp. 440–453
- [16] Sun, J., Sun, J.: ‘Real-time crash prediction on urban expressways: identification of key variables and a hybrid support vector machine model’, *IET Intell. Transp. Syst.*, 2016, **10**, (5), pp. 331–337
- [17] Abdel-Aty, M., Wang, L.: ‘Reducing real-time crash risk for congested expressway weaving segments using ramp metering’. 5th IEEE Int. Conf. Models and Technologies for Intelligent Transportation, Naples, Italy, 2017
- [18] Wang, X., Hadizuzzaman, M., Fang, J., et al.: ‘Optimal ramp metering control for weaving segments considering dynamic weaving capacity estimation’, *J. Transp. Eng.*, 2014, **140**, (11), article ID: 04014057
- [19] Papageorgiou, M., Papamichail, I.: ‘Overview of traffic signal operation policies for ramp metering’, *Transp. Res. Rec.*, 2008, **2047**, (2047), pp. 28–36
- [20] Chen, D., Ahn, S.: ‘Variable speed limit control for severe non-recurrent freeway bottlenecks’, *Transp. Res. Part C Emerg. Technol.*, 2015, **51**, pp. 210–230
- [21] Wang, L., Abdel-Aty, M., Lee, J.: ‘Implementation of active traffic management strategies for safety on congested expressway weaving segments’, *Transp. Res. Rec.*, 2017, **2635**, (2635), pp. 28–35
- [22] Sun, J., Zhang, S., Tang, K.S.: ‘Online evaluation of an integrated control strategy at on-ramp bottleneck for urban expressways in Shanghai’, *IET Intell. Transp. Syst.*, 2014, **8**, (8), pp. 648–654
- [23] Daganzo, C.F., Cassidy, M.J.: ‘Effects of high occupancy vehicle lanes on freeway congestion’, *Transp. Res. B. Methodol.*, 2008, **42**, (10), pp. 861–872
- [24] Lou, Y.: ‘A unified framework of proactive self-learning dynamic pricing for high-occupancy/toll lanes’, *Transportmetrica A: Transport Science*, 2013, **9**, (3), pp. 205–222
- [25] Kim, W., Liu, Y., Chang, G.L.: ‘Advanced traffic management system: integrated multicriterion system for assessing detour decisions during

- [26] nonrecurrent freeway congestion', *Transp. Res. J.*, 2012, **2324**, (2324), pp. 91–100
- [27] Daganzo, C.F., Laval, J., Muñoz, J.C.: 'Ten strategies for freeway congestion mitigation with advanced technologies' (University of California, Oakland, CA, US, 2002)
- [28] Wang, Y., Ma, W., Wang, Y., et al.: 'Dynamic lane assignment approach for freeway weaving segment operation', *Transp. Res. Rec.*, 2015, **2484**, pp. 39–49
- [29] Zhao, J., Ma, W.J., Liu, Y., et al.: 'Optimal operation of freeway weaving segment with combination of lane assignment and on-ramp signal control', *Transportmetrica A Transp. Sci.*, 2016, **12**, (5), pp. 413–435
- [30] Nagai, R., Nagatani, T., Taniguchi, N.: 'Traffic states and jamming transitions induced by a bus in two-lane traffic flow', *Physica A*, 2005, **350**, (2–4), pp. 548–562
- [31] Du, L., Song, G.J., Wang, Y.M., et al.: 'Traffic events oriented dynamic traffic assignment model for expressway network: a network flow approach', *IEEE Intell. Transp. Syst. Mag.*, 2018, **10**, (1), pp. 107–120
- [32] Tang, T.Q., Li, C.Y., Huang, H.J., et al.: 'A new fundamental diagram theory with the individual difference of the driver's perception ability', *Nonlinear Dyn.*, 2012, **67**, (3), pp. 2255–2265
- [33] Tang, T.Q., Wang, Y.P., Yang, X.B., et al.: 'A new car-following model accounting for varying road condition', *Nonlinear Dyn.*, 2012, **70**, (2), pp. 1397–1405
- [34] Knoop, V.L., Hoogendoorn, S.P.: 'Empirics of a generalized macroscopic fundamental diagram for urban freeways', *Transp. Res. Rec.*, 2013, **2391**, (2391), pp. 133–141
- [35] Zhao, J., Liu, Y., Wang, T.: 'Increasing signalized intersection capacity with unconventional use of special width approach lanes', *Comput.-Aided Civ. Infrastruct. Eng.*, 2016, **31**, (10), pp. 794–810
- [36] Zhao, J., Ma, W.J., Xu, H.J.: 'Increasing the capacity of the intersection downstream of the freeway off-ramp using presignals', *Comput.-Aided Civ. Infrastruct. Eng.*, 2017, **32**, (8), pp. 674–690
- [37] Hou, Y., Edara, P., Sun, C.: 'Traffic flow forecasting for urban work zones', *IEEE Trans. Intell. Transp. Syst.*, 2015, **16**, (4), pp. 1761–1770
- [38] Wang, L., Abdel-Aty, M., Shi, Q., et al.: 'Real-time crash prediction for expressway weaving segments', *Transp. Res. Part C-Emerg. Technol.*, 2015, **61**, pp. 1–10
- [39] Jin, W.L.: 'A multi-commodity Lighthill–Whitham–Richards model of lane-changing traffic flow', *Transp. Res. Part B-Methodol.*, 2013, **57**, pp. 361–377
- [40] Wan, X., Jin, P.J., Yang, F., et al.: 'Modeling vehicle interactions during merge in congested weaving section of freeway ramp', *Transp. Res. Rec.*, 2014, **2421**, (2421), pp. 82–92
- [41] Ros, B.G., Knoop, V.L., van Arem, B., et al.: 'Empirical analysis of the causes of stop-and-go waves at sags', *IET Intell. Transp. Syst.*, 2014, **8**, (5), pp. 499–506
- [42] Ci, Y.S., Wu, L.N., Ling, X.Z., et al.: 'Operation reliability for on-ramp junction of urban freeway', *J. Central South Univ. Technol.*, 2011, **18**, (1), pp. 266–270
- [43] Kong, L.P., Li, X.G., Lam, W.H.K.: 'Traffic dynamics around weaving section influenced by accident: cellular automata approach', *Int. J. Mod. Phys. C*, 2015, **26**, (3), article ID: 1550026
- [44] Tang, T.Q., Huang, H.J., Shang, H.Y.: 'A new pedestrian-following model for aircraft boarding and numerical tests', *Nonlinear Dyn.*, 2012, **67**, (1), pp. 437–443
- [45] Darwish, S.M.: 'Empowering vehicle tracking in a cluttered environment with adaptive cellular automata suitable to intelligent transportation systems', *IET Intell. Transp. Syst.*, 2017, **11**, (2), pp. 84–91
- [46] Ben, X.Y., Huang, X.F., Zhuang, Z.Y., et al.: 'Agent-based approach for crowded pedestrian evacuation simulation', *IET Intell. Transp. Syst.*, 2013, **7**, (1), pp. 55–67
- [47] Pascale, A., Nicoli, M., Deflorio, F., et al.: 'Wireless sensor networks for traffic management and road safety', *IET Intell. Transp. Syst.*, 2012, **6**, (1), pp. 67–77
- [48] Yin, B., Dridi, M., El Moudni, A.: 'Traffic network micro-simulation model and control algorithm based on approximate dynamic programming', *IET Intell. Transp. Syst.*, 2016, **10**, (3), pp. 186–196
- [49] Wang, R.L., Jiang, R., Liu, M.Z.: 'Effects of passing lanes on highway traffic flow', *Int. J. Mod. Phys. C*, 2007, **18**, (12), pp. 1865–1883
- [50] Rassafi, A.A., Davoodnia, P., Pourmoalem, N.: 'Modeling traffic flow on urban highways: the application of cellular automata and nested logit', *Arab. J. Sci. Eng.*, 2012, **37**, (6), pp. 1557–1570
- [51] Lan, L.W., Chiou, Y.C., Lin, Z.S., et al.: 'A refined cellular automaton model to rectify impractical vehicular movement behavior', *Physica A*, 2009, **388**, (18), pp. 3917–3930
- [52] Lv, W., Song, W.G., Fang, Z.M.: 'Three-lane changing behaviour simulation using a modified optimal velocity model', *Physica A*, 2011, **390**, (12), pp. 2303–2314
- [53] TRB: 'Highway capacity manual 2010' (Transportation Research Board, Washington, DC, US, 2010)
- [54] Rickert, M., Nagel, K., Schreckenberg, M., et al.: 'Two lane traffic simulations using cellular automata', *Physica A*, 1996, **231**, (4), pp. 534–550
- [55] MOHURD: 'Code for design of urban road engineering' (Ministry of Housing and Urban-Rural Development of the People's Republic of China (MOHURD), Beijing, China, 2012)
- [56] Zhao, J., Liu, Y.: 'Safety evaluation of intersections with dynamic use of exit-lanes for left-turn using field data', *Accident Anal. Prev.*, 2017, **102**, pp. 31–40
- [57] Zhao, J., Li, P., Zheng, Z., et al.: 'Analysis of saturation flow rate at tandem intersections using field data', *IET Intell. Transp. Syst.*, 2018, **12**, (5), pp. 394–403
- [58] Ma, C., Hao, W., Wang, A., et al.: 'Developing a coordinated signal control system for urban ring road under the vehicle-infrastructure connected environment', *IEEE Access.*, 2018, **6**, pp. 52471–52478
- [59] Wang, Y., Wenjuan, E., Tang, W., et al.: 'Automated on-ramp merging control algorithm based on internet-connected vehicles', *IET Intell. Transp. Syst.*, 2013, **7**, (4), pp. 371–379
- [60] Learn, S., Ma, J., Raboy, K., et al.: 'Freeway speed harmonisation experiment using connected and automated vehicles', *IET Intell. Transp. Syst.*, 2018, **12**, (5), pp. 319–326